

# Heterogeneous Mercury Reaction on a Selective Catalytic Reduction (SCR) Catalyst

Yujin Eom · Seok Ho Jeon · Thanh An Ngo ·  
Jinsoo Kim · Tai Gyu Lee

Received: 24 August 2007 / Accepted: 16 October 2007 / Published online: 14 November 2007  
© Springer Science+Business Media, LLC 2007

**Abstract** The heterogeneous mercury reaction mechanism, reactions among elemental mercury ( $\text{Hg}^0$ ) and simulated flue gas across laboratory-scale selective catalytic reduction (SCR) reactor system was studied. The surface of SCR catalysts used in this study was analyzed to verify the proposed reaction pathways using transmission electron microscopy with energy dispersive X-ray analyses (TEM-EDX) and X-ray photoelectron spectroscopy (XPS). The Langmuir–Hinshelwood mechanism was proven to be most suitable explaining first-layer reaction of  $\text{Hg}^0$  and HCl on the SCR catalyst. Once the first layer is formed, successive layers of oxidized mercury ( $\text{HgCl}_2$ ) are formed, making a multi-layer structure.

**Keywords** Heterogeneous mercury reaction · Selective catalytic reduction · Coal-fired power plant · Langmuir–Hinshelwood

## 1 Introduction

Recently, the U.S. Environmental Protection Agency (EPA) announced the Clean Air Mercury Rule (CAMR), which permanently caps mercury emissions from coal-fired power plants and establishes a mercury cap-and-trade

program [1]. CAMR will be implemented in two phases: first cap of 38 tons in 2010 and second cap of 15 tons in 2018. By the end of the second cap, the emission level is required to be reduced by 70% to the emission level in 1999. Out of the three forms of Mercury in coal-fired flue gas: elemental ( $\text{Hg}^0$ ), oxidized ( $\text{Hg}^{2+}$ ), and particle-bound ( $\text{Hg}^{\text{P}}$ ) [2].  $\text{Hg}^{2+}$  and  $\text{Hg}^{\text{P}}$  are easy to remove from flue gas using a typical air pollutions control device (APCD). Since  $\text{Hg}^{2+}$  is soluble in water, wet flue gas desulfurization (FGD) can effectively remove  $\text{Hg}^{2+}$  [3–6]. Like other trace metals, Hg is vaporized and first exists as a gas-phase  $\text{Hg}^0$  once coal is combusted at high temperatures. It has been verified by an equilibrium calculation [7].  $\text{Hg}^0$ , however, is difficult to capture because of its high volatility and insolubility. Selective catalyst reduction (SCR) catalysts with  $\text{NH}_3$ /urea are effective in removing nitrous oxides ( $\text{NO}_x$ ) as well as oxidizing Hg in the flue gas of coal-fired power plants [8, 9]. If the amount of  $\text{Hg}^{2+}$  in the flue gas can be maximized on the upstream of a wet FGD, a low-cost option for the control of Hg from coal-fired power plants can be achieved. For this reason, the combination of SCR and wet scrubbers has been recognized as an effective way of controlling Hg emissions from coal-fired power plants using existing APCDs [10].

$\text{Hg}^0$  can undergo either homogeneous or heterogeneous reactions on the SCR reactor. SCR catalysts are believed to facilitate heterogeneous oxidation, which typically have faster reaction times than homogeneous oxidation [11, 12]. Recent studies have shown a wide range of observed results ranging from 0 to in excess of 95% Hg oxidation across the SCR units [10, 12, 13]. Nevertheless, the studies agree on two major points: (1) Higher HCl content in flue gases promotes Hg oxidation [9], and (2) the addition of  $\text{NH}_3$  to the SCR process decreases the Hg oxidation with a greater effect at higher space velocities [14]. Many researchers

---

Y. Eom · S. H. Jeon · T. G. Lee (✉)  
Department of Chemical Engineering, Yonsei University,  
134 Sinchon-dong, Seodaemun-gu, Seoul 120-749,  
Republic of Korea  
e-mail: teddy.lee@yonsei.ac.kr

T. A. Ngo · J. Kim  
Department of Chemical Engineering, Kyung Hee University,  
1 Sochen-ri, Giheung-eup, Yongin, Gyeonggi-do 449-701,  
Republic of Korea

have reported that the Hg oxidation across SCR units significantly varies depending on many factors, such as coal type [9, 14], concentration of other species (i.e., HCl, NO<sub>x</sub>, and SO<sub>2</sub>) [13] in the flue gas, SCR catalyst type, and other operating conditions. However, the reactions crucial to the transformation of Hg<sup>0</sup> to Hg<sup>2+</sup> in the SCR reactor are not well understood. A number of researchers studying heterogeneous mercury oxidation have proposed several possibilities of the mechanism for mercury oxidation on SCR catalysts, but no one has been able to establish the dominant mechanism for catalytic mercury oxidation. In order to develop an efficient and economic catalyst, which carries out both mercury oxidation and NO<sub>x</sub> removal, surface-catalyzed mercury oxidation mechanism and kinetics must be researched and understood first.

In this study, laboratory-scale SCR reactor system capable of varying flue gas compositions and test conditions was set up in order to understand heterogeneous mercury oxidation reaction across SCR catalyst. Furthermore, detailed reaction routes and mercury reaction pathways are proposed based on the mercury concentration and speciation analysis, and are further proven by surface characterization of the catalyst.

## 2 Experimental

### 2.1 Apparatus

A schematic diagram of the system is shown in Fig. 1. The system consists of pre-heating and pre-mixing units, the Hg generation unit, the SCR reactor, and the on-line measurement unit. Gas cylinders of N<sub>2</sub>-diluted gaseous species were used instead of pure gases for some components (i.e., HCl/N<sub>2</sub>, NO/N<sub>2</sub>, and NH<sub>3</sub>/N<sub>2</sub>). The flow rate of each inlet

gas stream is carefully controlled using a mass flow controller (MFC). Then, the gas is passed through the static gas mixing section and enters the SCR reactor. All the gas transport line and mixing section are made of stainless steel to minimize the corrosive effect of the acidic gases. Proper pre-heating and mixing of the gas are vital in simulating the SCR reactor conditions. The Hg generation unit consists of an Hg permeation tube surrounded by a temperature-controlled water bath, which was used to generate Hg<sup>0</sup> vapor. Hg<sup>0</sup> vapor is carried by an N<sub>2</sub> stream into the top of the SCR reactor (1.8 cm inner diameter and 40 cm in length, Quartz). The gaseous effluent stream exiting from the SCR reactor was passed to an on-line Hg analyzer (VM 3000, Mercury Ins.) and NO<sub>x</sub> analyzer (9110EH, Teledyne Analytical Ins.), and for the Hg speciation tests, the Ontario Hydro Method (ASTM D6784, 2002) was used [15]. Hg<sup>2+</sup> was collected in first three impingers containing an aqueous potassium chloride solution. Hg<sup>0</sup> was collected in the fourth and the next three impingers containing an aqueous acidic solution of hydrogen peroxide and aqueous acidic solutions of potassium permanganate, respectively. Samples were then recovered, digested, and analyzed using CVAAs (cold vapor atomic absorption)-type Hg analyzer (RA-915+, Lumex Ltd.). Both temperature controller and heating tape were used to maintain the temperature of exhaust gases high enough to prevent Hg condensation.

### 2.2 Test Conditions in the SCR Reactor

A commercial SCR catalyst with a vanadia/titania formulation with a honeycomb configuration was used in the study. A small piece (0.9 cm for both sides and 17.2 cm in length) of the catalyst sample was placed into the catalyst

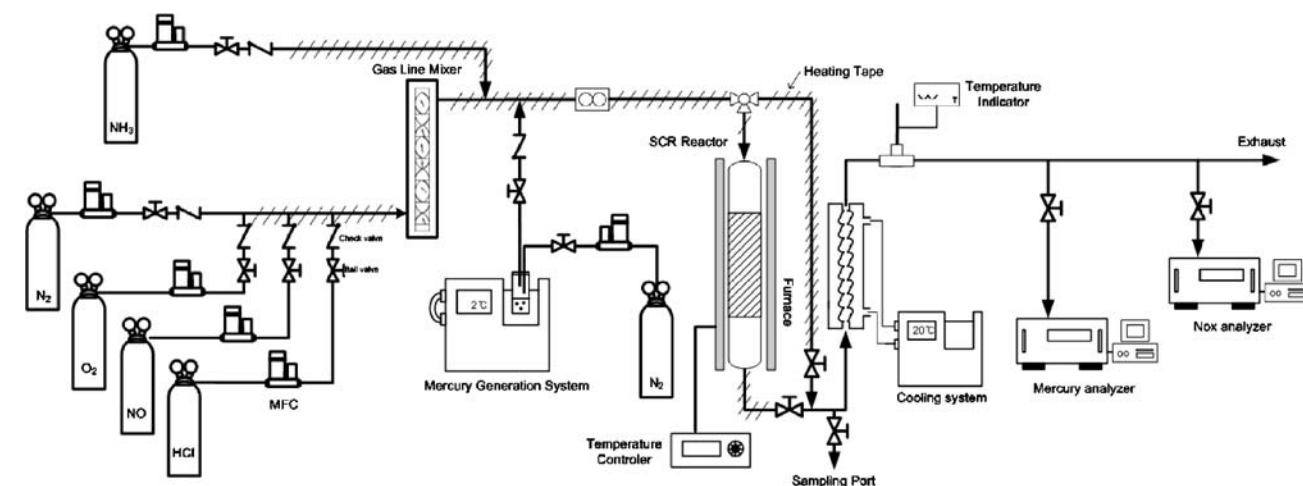


**Fig. 1** A schematic diagram of the SCR reactor system

compartment of the SCR reactor. A series of six tests were conducted in order to understand the mechanism of the mercury reaction.

On the SCR catalyst, reactions among Hg, the SCR catalyst, O<sub>2</sub>, and HCl gas were carefully analyzed. Although HCl is believed to be the most vital factor in Hg oxidation of the SCR catalyst, the effect of NH<sub>3</sub> was also tested by introducing it into the inlet stream. The compositions of the simulated flue gases used in this study are shown in Table 1. All tests were conducted at 350 °C with a constant total flue gas flow rate of 2,000 cm<sup>3</sup>/min under standard conditions (T = 25 °C, P = 101.3 kPa). The calculated space velocity for the tests was 4,000 h<sup>-1</sup>, similar to those used in the field. NO<sub>x</sub> and Hg<sup>0</sup> concentrations measured at the outlet of the reactor showed that the concentrations reached a steady value.

### 2.3 Catalyst Characterization

The identification of crystallinity and its purity in the SCR catalyst was carried out by X-ray diffraction (XRD, Miniflex, Rigaku). XRD patterns were obtained in the 2 $\theta$  range from 20 to 100 with nickel filtered Cu K $\alpha$  radiation ( $\lambda$  = 1.54 Å). The BET surface area was determined by N<sub>2</sub> adsorption isotherms at 77 K using a Micromeritics ASAP 2010 analyzer. TEM-EDX (JEM-2100, JEOL) was used to examine the morphology and chemical composition of the SCR catalyst. The chemical bonding modification of the catalyst surface was monitored using XPS (ESCALAB 220I-XL, VG Scientifics Ins.) with a monochromatic Al K $\alpha$  source.

## 3 Results and Discussion

### 3.1 Catalyst Property

The heterogeneous reaction between Hg and the SCR catalyst was studied under various simulated flue gas conditions. The catalyst used in this study is vanadium

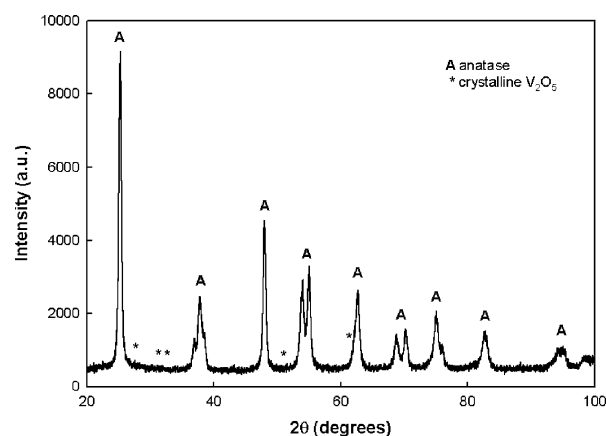


**Fig. 2** XRD patterns of the initial V<sub>2</sub>O<sub>5</sub>–WO<sub>3</sub>/TiO<sub>2</sub> catalyst (anatase diffraction peaks labeled, ICDD card No. 21-1272)

pentoxide (V<sub>2</sub>O<sub>5</sub>)—tungsten trioxide (WO<sub>3</sub>) on titanium dioxide (TiO<sub>2</sub>), which is a widely used commercial Ti/V-based SCR catalyst. As shown in Fig. 2, the catalyst used in this study has the crystallinity of TiO<sub>2</sub> in its anatase form. Since the crystallinity of the activated component, V<sub>2</sub>O<sub>5</sub>, is not observed (Fig. 2), it can be concluded that V<sub>2</sub>O<sub>5</sub> is evenly dispersed in TiO<sub>2</sub>. TEM images in Fig. 3 confirm the even dispersion of V<sub>2</sub>O<sub>5</sub> on the surfaces of TiO<sub>2</sub>. Here, the crystalline particles are between 20 and 100 nm. The previous study suggests that the surface layer

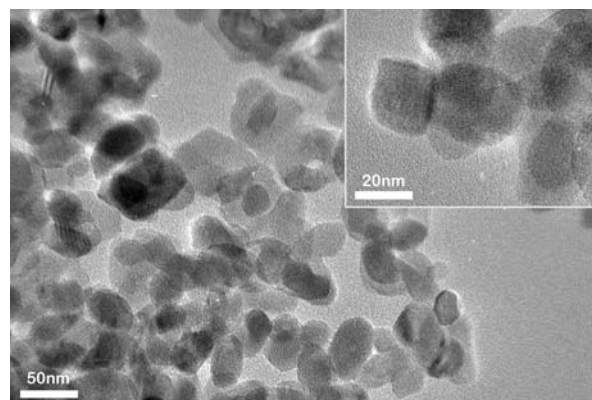


**Fig. 3** TEM image of the new V<sub>2</sub>O<sub>5</sub>–WO<sub>3</sub>/TiO<sub>2</sub> catalyst

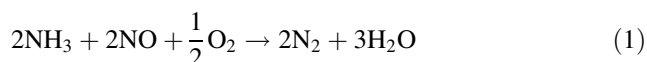
**Table 1** List of experiments and the composition of the simulated flue gas

Test No.	Flue gas compositions				
	O <sub>2</sub> (%)	HCl (ppm)	NO (ppm)	NH <sub>3</sub> (ppm)	Hg <sup>0</sup> (μg /m <sup>3</sup> )
1. Hg <sup>0</sup> + N <sub>2</sub> + SCR catalyst					38.9
2. Hg <sup>0</sup> + N <sub>2</sub> + NH <sub>3</sub> + NO + SCR catalyst			400	360	37.7
3. Hg <sup>0</sup> + N <sub>2</sub> + O <sub>2</sub> + SCR catalyst	6				36.9
4. Hg <sup>0</sup> + N <sub>2</sub> + O <sub>2</sub> + NH <sub>3</sub> + NO + SCR catalyst	6		400	360	37.3
5. Hg <sup>0</sup> + N <sub>2</sub> + O <sub>2</sub> + HCl + SCR catalyst	6	50			36.3
6. Hg <sup>0</sup> + N <sub>2</sub> + O <sub>2</sub> + HCl + NH <sub>3</sub> + NO + SCR catalyst	6	50	400	360	38.7

is primarily tungsten oxide, and the vanadia is generally below 1 nm [16]. The vanadia content of the catalyst detected by EDX was 2 wt.%, consistent with the precursor composition. The BET surface area of the catalyst was 61 m<sup>2</sup>/g, and its average pore diameter was 151 Å.

### 3.2 Heterogeneous Mercury Reaction on the SCR Catalyst

The tests were carried out following the same procedure as for Table 1, and NO<sub>x</sub> reduction reached 80–90% in all tests other than Test #2. For the second experiment (Test #2), no NO<sub>x</sub> reduction was observed, since the O<sub>2</sub> required for NO<sub>x</sub> reduction (Eq. 1) is not present.



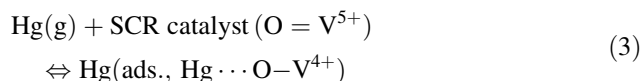
The influence each component of the flue gas has on the Hg oxidation and retention was determined by adding only one of the components to the flue gas, thus enabling the observation of each component's effect alone possible. The tests were done using a new catalyst each time, and three replicates were done for each test to ensure its reproducibility. Except for the flue gas components, all other parameters in the test, such as the SCR reactor temperature and space velocity, were the same as in actual coal-fired power plants.

Figure 4 shows the Hg<sup>0</sup> concentration profile at the inlet and outlet of the SCR reactor for each test (Table 1). Mercury speciation results are shown in Table 2. The Hg<sup>0</sup> removal efficiency,  $\eta$ , is defined as follows:

$$\eta = \frac{\text{Hg}_{\text{in}}^0 - (\text{Hg}_{\text{out}}^0 + \text{Hg}_{\text{out}}^{2+})}{\text{Hg}_{\text{in}}^0} \times 100 \quad (2)$$

where Hg<sub>in</sub><sup>0</sup> is the gas phase concentration of Hg<sup>0</sup> into the SCR reactor, Hg<sub>out</sub><sup>0</sup> the concentration of Hg<sup>0</sup> in the flow stream out of the reactor, and Hg<sub>out</sub><sup>2+</sup> the concentration of Hg<sup>2+</sup> in the flow stream out of the reactor.

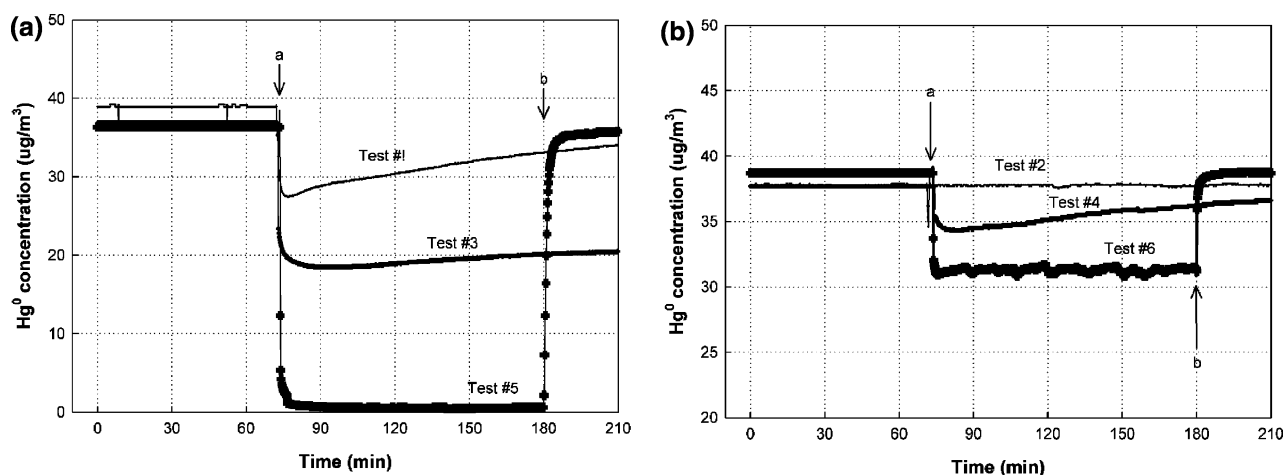
As shown in Fig. 4a, when N<sub>2</sub> is used without other components, the Hg removal efficiency of the SCR catalyst is 14.1% and gradually decreases.



XRD and TEM analysis show that the catalyst used in this study has a monomeric vanadyl layer of O=V<sup>5+</sup> on the TiO<sub>2</sub> surfaces. Thus, as suggested by Eq. 3, gaseous Hg is adsorbed onto the active sites, O=V<sup>5+</sup>, and becomes HgL O–V<sup>4+</sup>(ads.). This is confirmed by the XPS analysis.

In XPS analysis, peak separation among three types of mercury; Hg<sup>0</sup> 4f<sub>7/2</sub> (99.5–100.0 eV), HgO (100.5–101.1 eV) and HgCl<sub>2</sub> (101.4 eV) is difficult because of the small differences in their bonding energies [17, 18]. Furthermore, the chemical structure of the V<sub>2</sub>O<sub>5</sub>–WO<sub>3</sub>/TiO<sub>2</sub> catalyst is complex, which makes it more difficult to analyze. Thus, the O 1s peak was used to analyze the results.

Referring to the bonding energy scale of O 1s from the study of Danielle et al. (Fig. 5), the bonding energy values of four different types of O 1s peaks can be judged from the difference in the electronegativity of the elements [19]. Figure 6 shows the peak separation of the O 1s-line for SCR catalyst surface after 0, 10, and 48 h under the Test #1 flue gas conditions in Table 1. Component a, the O 1s peak with the binding energy of 529.9 eV, represents the O 1s-level of oxygen atoms O<sup>2–</sup> in the lattice. Free oxide surfaces in contact with the atmosphere are always hydrated, often containing water molecules and hydroxyl groups.

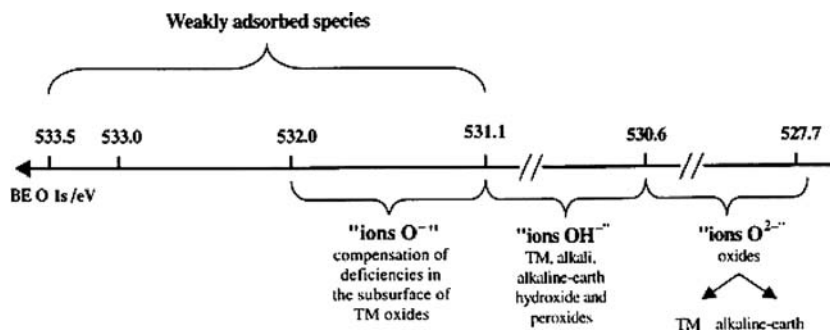


**Fig. 4** Real-time Hg<sup>0</sup> concentration at the exit of the SCR reactor for each test (Table 1) using an on-line Hg<sup>0</sup> analyzer: (a) without NH<sub>3</sub> and NO and (b) with NH<sub>3</sub> and NO. At point a, once the Hg vapor flow

stabilized, it was switched from the blank line to the SCR reactor. At point b, the flow was switched back to the blank line to check its initial Hg concentration (Tests #5 and #6)

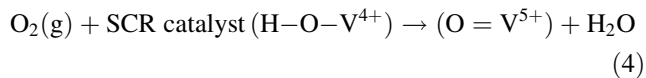
**Table 2** Mercury speciation results using the Ontario Hydro Method

	Average ( $\mu\text{g}/\text{m}^3$ ) and standard deviation											
	Test #1		Test #2		Test #3		Test #4		Test #5		Test #6	
	Avg.	SD	Avg.	SD	Avg.	SD	Avg.	SD	Avg.	SD	Avg.	SD
Inlet $\text{Hg}^0$ concentration	37.3	2.0	36.2	1.3	37.5	0.6	36.7	1.3	37.2	1.5	37.3	1.2
Outlet $\text{Hg}^0$ concentration	32.0	2.2	36.6	1.5	21.5	0.5	35.5	1.3	2.1	2.1	33.0	1.5
Outlet $\text{Hg}^{2+}$ concentration	0.0	0.0	0.0	0.0	0.0	0.1	0.4	0.1	3.3	0.5	0.5	0.2
$\text{Hg}^0$ removal efficiency (%)	14.7	1.2	0.0	0.0	42.6	2.0	3.0	0.3	91.2	4.6	11.1	1.9

**Fig. 5** A binding energy scale for the O 1s peak [19]

Component b represents the single M-OH (M indicates Ti, V, or W) and double OH-M-OH peaks in the region of O 1s with 530.5 eV. Component c, the peak in region 531.7 eV, corresponds to the weakly adsorbed species and  $\text{O}^-$  oxygen state. As shown in Fig. 6c, the weakly adsorbed Hg peak of  $\text{HgL O-V}^{4+}(\text{ads.})$  is observed from the O 1s results for the catalyst after 48 h of tests. Component d in the 532.6 eV represents  $\text{H}_2\text{O}$  molecules. When  $\text{NH}_3$  is added to the gas stream in Test #2, however, the efficiency of Hg removal is nearly at zero (Fig. 4b). The result in Test #2 strongly suggests that both  $\text{NH}_3$  and  $\text{Hg}^0$  adsorb onto the same active sites of the SCR catalyst and that the reaction rate of  $\text{NH}_3$  is much faster than the reaction rate of  $\text{Hg}^0$ .

When 6%  $\text{O}_2$  is introduced (Test #3), a much higher mercury efficiency of 40.7% is observed, and the result of the Hg speciation analysis confirms that Hg is adsorbed strongly to the catalyst (Table 2). The homogeneous reaction of  $\text{Hg}^0$  and  $\text{O}_2$  is unattainable to form  $\text{HgO}$  (g) at 350 °C [20, 21]. The adsorption mechanism between Hg and the SCR catalyst is mentioned above (Eq. 3), and the effect of the addition of  $\text{O}_2$  on the surface of the  $\text{V}_2\text{O}_5$ - $\text{WO}_3/\text{TiO}_2$  catalyst can be written:



Equation 4 shows that Hg removal efficiency is increased because  $\text{O}_2$  activates more active sites of the SCR catalyst. With the introduction of  $\text{NH}_3$  and NO (Test #4), the Hg removal efficiency significantly decreases. The gradual decrease in the efficiency of Hg removal in respect to time,

despite of the high Hg removal efficiency, is because sites with Hg adsorbed can no longer be active as in Eq. 3.

As shown in Fig. 4a, a high Hg removal efficiency of the SCR catalyst in the presence of HCl is observed (Test #5). Furthermore, the Hg removal efficiency remains constant throughout the entire reaction time. This suggests that a reactant ratio of HCl and  $\text{NH}_3$  exists in this competitive reaction. Although the Hg removal efficiency decreases with the presence of  $\text{NH}_3$ , it remains constant as the reaction time increases. The results of the speciation analysis show that only small amounts of  $\text{Hg}^{2+}$  are observed, and most of it is adsorbed on the surfaces of the catalyst. In case of tests #5 and #6, a constant mercury removal rate was observed in spite of limited number of active sites, suggesting that after the active sites were first occupied with mercury, the successive mercury was removed by adsorption onto the multi-layer of mercury formed on the catalyst's surface. According to Niksa and Fujiwara's [9] proposal of reaction mechanism, HCl adsorbs to the surface of  $\text{V}_2\text{O}_5$  and gaseous  $\text{Hg}^0$  reacts to this by Hg oxidation; however, Niksa and Fujiwara's proposal cannot explain the adsorption of  $\text{Hg}^0$  observed in the result of this research as well as in the results of Eswaran and Stinger's [22], and Senior's research [23]. On the other hand, Senior's proposal of reaction mechanism between adsorbed  $\text{Hg}^0$  and gaseous HCl is also refuted by the HCl adsorption test of this research. To test the adsorption of HCl, a gas stream without Hg was passed through the SCR catalyst, and then Hg without HCl was passed through. It vastly increased the Hg removal efficiency, which confirms



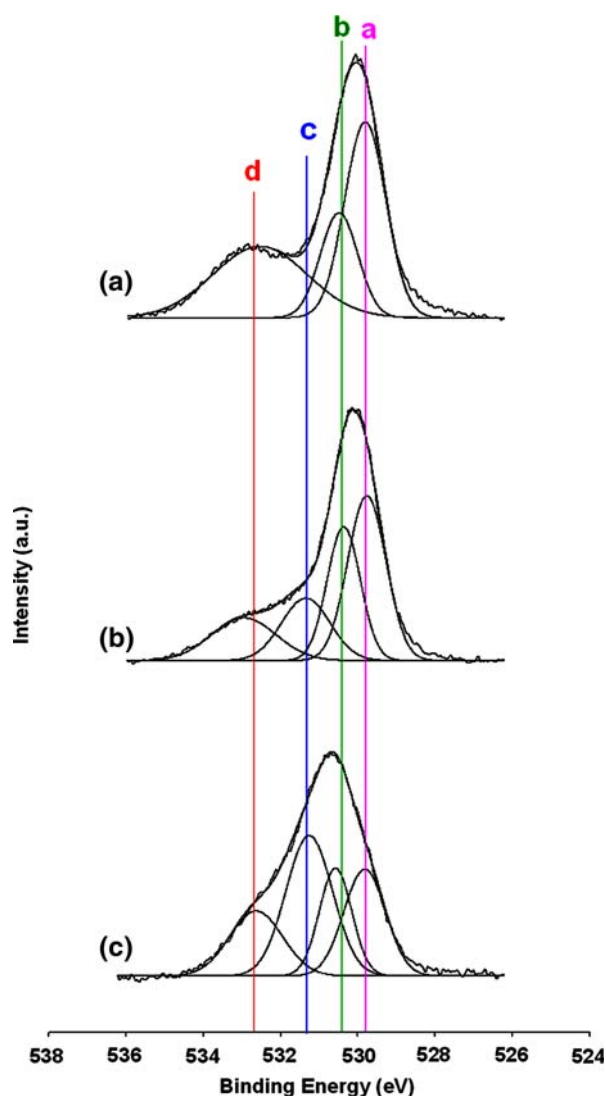
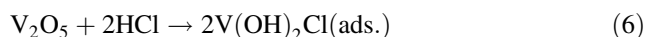
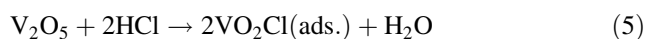
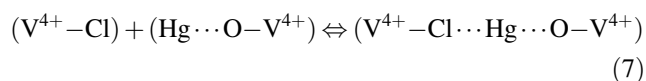


**Fig. 6** XPS spectra of the O 1s peak of (a) SCR catalyst, (b) SCR catalyst reacted with  $\text{Hg}^0$  for 10 h, and (c) 48 h

that HCl is, in fact, adsorbed onto the surface of the SCR catalyst. The  $\text{V}_2\text{O}_5\text{-WO}_3/\text{TiO}_2$  catalyst reacts with HCl according to following reactions:



Hg and chlorine species that are adsorbed onto the catalyst react according to the following reaction:



The Langmuir–Hinshelwood and Eley–Rideal mechanisms are two possible adsorption mechanisms that can explain the first layer of  $\text{Hg}^0$  and HCl reaction on the surface of SCR catalysts [9, 24, 25]. The Langmuir–Hinshelwood mechanism suggests that both  $\text{Hg}^0$  and chlorine molecules

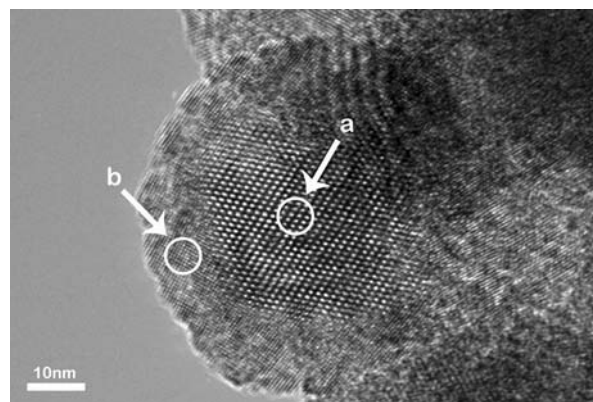


**Fig. 7** TEM image of the used  $\text{V}_2\text{O}_5\text{-WO}_3/\text{TiO}_2$  catalyst from Test #6 (a: crystalline  $\text{TiO}_2$ , b: adsorbing molecules)

are adsorbed onto surfaces. The Eley–Rideal mechanism proposes that only one species is adsorbed while the other species reacts with the one that is adsorbed. In other words, the key to the initial reaction pathway of  $\text{Hg}^0$  and HCl is whether HCl is adsorbed onto the surface of the catalyst or not. Based on the results from Test #1 to Test #6 discussed, the Langmuir–Hinshelwood mechanism is proven to be the most suitable mechanism for first layered catalysts. Once the first layer is formed (Eq. 3), successive layers of oxidized mercury ( $\text{HgCl}_2$ ) are formed with covalent and/or donor-acceptor bonds. If such a multi-layer is formed, the initial reaction of Hg with HCl on the catalyst surface cannot be explained by the Eley–Rideal mechanism, although it is suggested by particles that are observed on the TEM image (Fig. 7) of the SCR catalyst from Test #6. As shown in Fig. 7, a multi-layer of adsorbed molecules (b) is formed on the surface of the  $\text{TiO}_2$  (a).

## 4 Conclusions

It was observed that Hg is weakly adsorbed ( $\text{Hg}\cdots\text{O}-\text{V}^{4+}(\text{ads.})$ ) onto the catalyst surface without any oxidant, which was confirmed by XPS analysis. Results show that the Hg removal efficiency is increased by passing HCl through the SCR catalyst first, and then passing Hg vapor without HCl through the catalyst. This result proves that the chlorine species in HCl is adsorbed onto the surface of the SCR catalyst. Furthermore, it suggests that both the Hg and chlorine species are adsorbed onto the SCR catalyst and undergo heterogeneous reactions with each other. Therefore, the formation of the first layer of Hg with the HCl complex on the surface of the catalyst follows the Langmuir–Hinshelwood mechanism. Once the first layer is formed, successive multi-layers of oxidized mercury ( $\text{HgCl}_2$ ) are formed with covalent and/or donor-acceptor bonds. The course of the research now is to examine the

mechanism of the heterogeneous mercury reaction with the SCR catalyst under more complex simulated flue gas and to study kinetics.

**Acknowledgements** This work was supported by grant No. (R01-2006-000-10007-0) from the Basic Research Program of the Korea Science & Engineering Foundation and by Ministry of Environment as the Eco-technopia 21 project (No. 2007-01003-0059-0).

## References

1. <http://www.epa.gov/air/mercuryrule/>
2. Galbreath K, Zygarlicke C (1996) *Environ Sci Technol* 30:2421
3. Serre S, Silcox G (2000) *Ind Eng Chem Res* 39:1723
4. Pavlish J, Sondreal E, Mann M, Olson E, Galbreath K, Laudal E, Benson S (2003) *Fuel Proc Technol* 82:89
5. Galbreath KC, Zygarlicke CJ (2000) *Fuel Process Technol* 65–66:289
6. Lee TG, Hedrick E, Biswas P (2002) *J Air Waste Manage Assoc* 52:1316
7. Senior CL, Bool LE, Huffman GP, Huggins FE, Shah N, Sarofim A, Olmez I, Zeng T (1997) Proceedings of the 90th Air & Waste Management Association annual meeting. Toronto, Canada
8. Lietti L, Ramis G, Berti F, Toledo G, Robba D, Busca G, Forzatti D (1998) *Catal Today* 42:101
9. Niksa S, Fujiwara N (2005) *J Air Waste Manage Assoc* 55:1866
10. Richardson C, Machalek T, Miller S, Dene C, Chang R (2002) *J Air Waste Manage Assoc* 52:941
11. Srivastava R, Hutson N, Martin B, Princiotta F, Staudt J (2006) *Environ Sci Technol* 40:1385
12. Laudal DL, Thompson JS, Pavlish JH, Brickett L, Chu P, Srivastava RK, Lee CW, Kilgroe J (2003) *Environ Manage* 1:16
13. Glenn AN, Hongqun Y, Robert CB, Dennis LL, Grant ED, John E (2003) *Fuel* 82:107
14. Carl R, Tom M, Scott M, Chuck D, Ramsay C (2002) *J Air Waste Manage Assoc* 52:941
15. ASTM D6784 (2002) Annual book of ASTM standards, vol 11.03. ASTM International, PA
16. Jossena R, Heinea MC, Pratsinisa SE, Augustineb SM, Akhtarb MK (2007) *Appl Catal B* 69:181
17. Briggs D, Seah MP (1996) Practical surface analysis (Appendix 5). John Wiley & Sons, Inc., New York
18. Hutson ND, Attwood B, Schecke K (2007) *Environ Sci Technol* 41:1747
19. Dupin J, Gobeau D, Vinatier P, Levasseur A (2000) *Phys Chem Chem Phys* 2:1319
20. Galbreath KC, Zygarlicke CJ (1996) *Environ Sci Technol* 30:2421
21. Hal B, Schager P, Lindqvist O (1991) *Water Air Soil Pollut* 56:3
22. Eswaran S, Stenger H (2005) *Energy Fuels* 19:2328
23. Senior CL (2006) *J Air Waste Manage Assoc* 56:23
24. Pilling M, Seakins PW (1995) Reaction kinetics. Oxford Science Publications, New York
25. Niksa S, Fujiwara N (2005) *J Air Waste Manage Assoc* 55:930